High-sensitivity detection of TNT

Michael B. Pushkarsky*†, Ilya G. Dunayevskiy*, Manu Prasanna*, Alexei G. Tsekoun*, Rowel Go*, and C. Kumar N. Patel*‡§

*Pranalytica, Inc., 1101 Colorado Avenue, Santa Monica, CA 90401; and ‡Department of Physics and Astronomy, University of California, Los Angles, CA 90095

Contributed by C. Kumar N. Patel, November 6, 2006 (sent for review October 26, 2006)

We report high-sensitivity detection of 2,4,6-trinitrotoluene (TNT) by using laser photoacoustic spectroscopy where the laser radiation is obtained from a continuous-wave room temperature high-power quantum cascade laser in an external grating cavity geometry. The external grating cavity quantum cascade laser is continuously tunable over ≈400 nm around 7.3 μm and produces a maximum continuous-wave power of ≈200 mW. The IR spectroscopic signature of TNT is sufficiently different from that of nitroglycerine so that unambiguous detection of TNT without false positives from traces of nitroglycerine is possible. We also report the results of spectroscopy of acetylene in the 7.3-μm region to demonstrate continuous tunability of the IR source.

quantum cascade lasers | high-power lasers | continuous-wave operation | room temperature operation | TNT detection

Detection of illegally transported explosives has become important since the global rise in terrorism subsequent to the events of September 11, 2001. Although not a choice of suicide bombers, 2,4,6-trinitrotoluene (TNT) is a potent explosive for which techniques for detection on a person's body or in one's baggage is considered important for assuring safety of airports and air travel. As with detection of other similar compounds, such as chemical warfare agents, any detection scheme that claims to detect these targets must exhibit acceptable receiver operational characteristic (ROC) that assures detection at very low levels without an unacceptable level of false alarms (1, 2). The molecular mass of TNT ($C_7H_5N_3O_6$) is almost exactly identical to the molecular mass of nitroglycerine ($C_3H_5N_3O_9$) even though the chemical compositions of the two molecules are very different (TNT, 227.131 Da vs. nitroglycerine, 227.0872 Da). The nearly same molecular masses often lead to problems for unambiguous detection of TNT using techniques that rely on measuring the molecular mass of the species. On the other hand, the differences in the chemical structure between TNT and nitroglycerine lead to noticeably different infrared (IR) absorption signatures (3), making it possible to distinguish between the two. However, the detection of TNT in vapor phase is hampered by its low vapor pressure of $\approx 2 \times 10^{-4}$ torr at 25°C. In this work, we report on studies of detection of TNT by using room-temperature (RT) quantum cascade laser (QCL)-based photoacoustic spectroscopy (QCL-PAS). The high sensitivity afforded by laser-based photoacoustic spectroscopy (L-PAS) (4) shows that the vapor-phase detection of TNT at an ambient temperature of ≈25°C is possible.

Previously, CO and CO_2 lasers have been used for photoacoustic (PA) spectroscopic detection (3, 5) of vapors of explosives. However, both of these laser sources are step tunable, and neither of the lasers is able to access the strong absorption features of TNT that lie in the 6.0–7.5 μm region. Quantum cascade lasers (QCLs), with their continuous tunability, should be the right sources for the detection of TNT and other species that do not absorb strongly in the 9–11.5 μm region. Finally, the small size, simplicity, and potential long-term reliability of QCLs (as seen from the long-term reliability data on other semiconductor lasers) could make QCL-PAS a more desirable technique for the detection of TNT compared with that reported in a study (6) using an optical parametric oscillator with a zinc-germanium-phosphide nonlinear crystal pumped by a flash-lamp pumped Q-switched erbium-chromium doped yttrium-scandium-gallium-garnet laser at 2.8 μm.

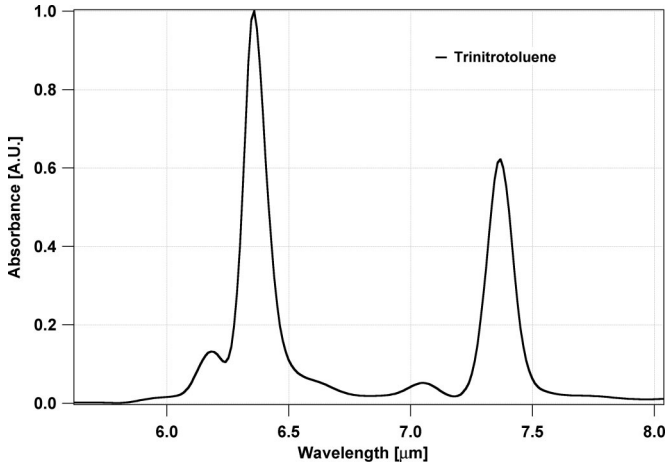

Fig. 1. FTIR absorption spectrum of TNT.

Results and Discussion

IR Absorption of TNT. TNT exhibits a strong but broad absorption feature at ≈7.3 μm (Fig. 1), a region that is not accessible using high-power lasers such as CO_2 lasers used for high-sensitivity PA detection of many gases including ammonia, SF_6, and ethylene. L-PAS derives its high detection sensitivity from a combination of factors that include remarkably low-noise PA detection technique and high continuous wave (CW) power laser radiation. The ability to distinguish the target species from potential interferents is afforded by tunability of the laser because of unique IR absorption fingerprints of each chemical compound (1). In the region of 7.3 μm, we have recently developed a relatively high-power CW/RT QCL source that is tunable over the spectral region where TNT has the absorption feature shown in Fig. 1.

Characteristics of the High-Power Continuously Tunable Laser. Fig. 2 shows the CW/RT laser output wavelength from the external grating cavity (EGC) QCL as a function of the grating tuning angle and representative Fourier transform IR (FTIR) spectra of

Author contributions: C.K.N.P. designed research; M.B.P., I.G.D., M.P., A.G.T., and R.G. performed research; M.B.P., I.G.D., and C.K.N.P. analyzed data; C.K.N.P. wrote the paper; and M.P. generated algorithms for continuous tuning of the external grating quantum cascade lasers.

The authors declare no conflict of interest.

Abbreviations: CDA, clean dry air; CW, continuous wave; EGC, external grating cavity; FTIR, Fourier transform IR; PA, photoacoustic; PAS, PA spectroscopy; L-PAS, laser-based PAS; QCL, quantum cascade laser; RT, room temperature.

†Present address: Daylight Solutions, 13029 Danielson Street, Suite 203, Poway, CA 92064.

§To whom correspondence should be sent at the * address. E-mail: patel@pranalytica.com.

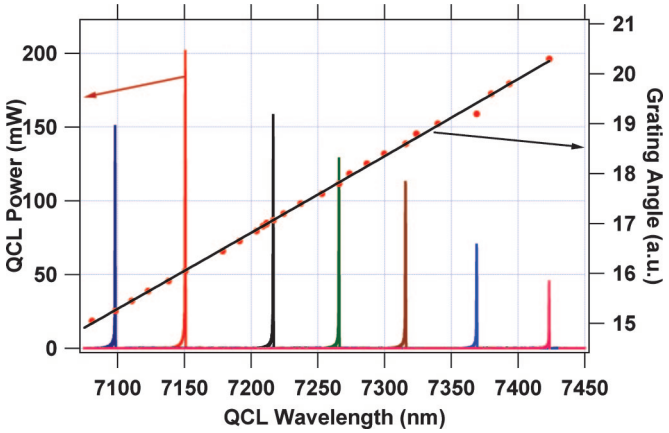

Fig. 2. Tuning characteristics of CW/RT operation of the 7.3-μm EGC QCL.

the output taken at seven grating angles. Continuous tunability over >350 nm has been demonstrated with highest single mode CW/RT power of >200 mW. We believe that with improved optics and optimized antireflection coatings on the grating side of the QCL gain chip and partially transmitting coating on the output side of the QCL, the tunability can be extended over a wider region with power outputs higher than those seen in Fig. 2. The single mode output as well as continuous tuning characteristics of our computer-controlled CW/RT EGC QCL were investigated at high resolution by using the FTIR spectrometer, which confirmed mode hop free operation and single frequency output with a linewidth of <600 MHz, limited by the FTIR resolution. Details are given in *Materials and Methods*.

Confirmation of Continuous Tuning Through PA Spectroscopy of Acetylene. Additional confirmation of narrow single frequency output and mode hop free tuning was obtained by carrying out spectroscopy of acetylene ($0\,0\,0\,1^1\,1^1$ band) shown in Fig. 3. The upper trace shows a simulated acetylene spectrum using HITRAN data (7) in the spectral region covering 7,250–7,450 nm. The lower trace shows PA spectra of 10 ppm acetylene in clean dry air (CDA) at a total pressure of 300 torr, obtained by using the radiation from the CW/RT ECG QCL that was tuned discreetly to 700 points in the spectral region. The very close similarity in shapes, locations, and intensities of the PA spectrum with the simulated spectrum confirms that the CW/RT ECG QCL, whose wavelength is controlled by the computer algorithm that simultaneously adjusts the grating angle, the QCL drive current, and the external cavity length, indeed produces mode hop free tunable power output over the range of wavelengths in Fig. 3.

We have looked at one specific absorption peak of acetylene from the spectrum shown in Fig. 3 to estimate the detectivity for

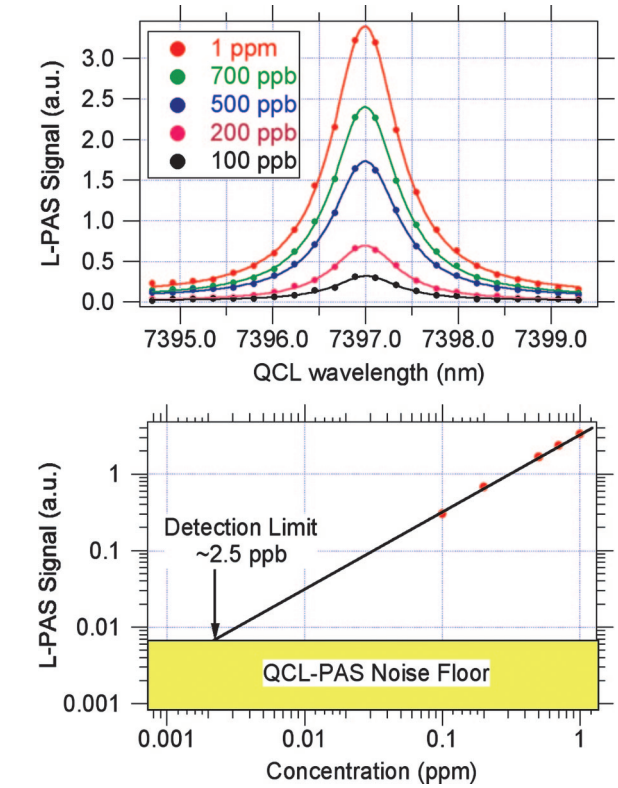

Fig. 4. QCL-PAS measurements for acetylene as a function of acetylene concentration.

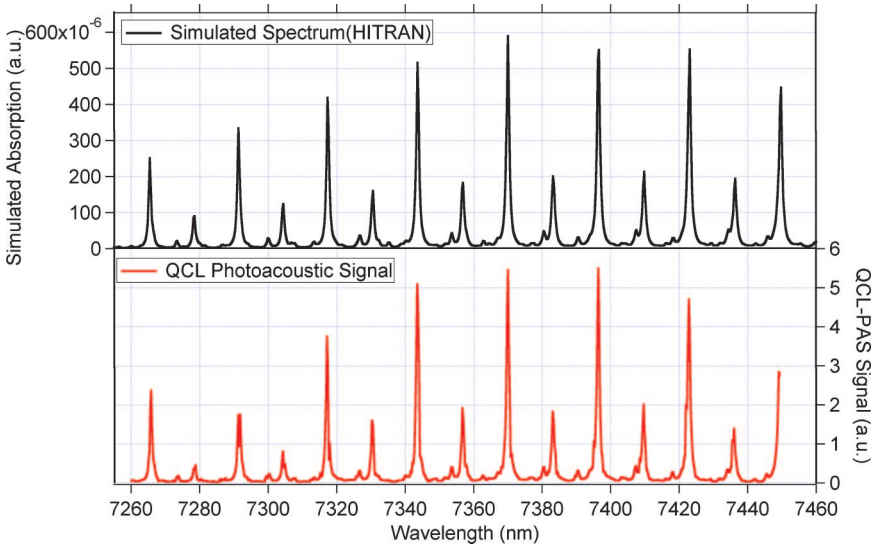

Fig. 3. High-resolution HITRAN simulated absorption spectrum of acetylene (*Upper*) and measured QCL-PAS spectrum of 10 ppm acetylene in CDA (*Lower*) at a total pressure of 300 torr.

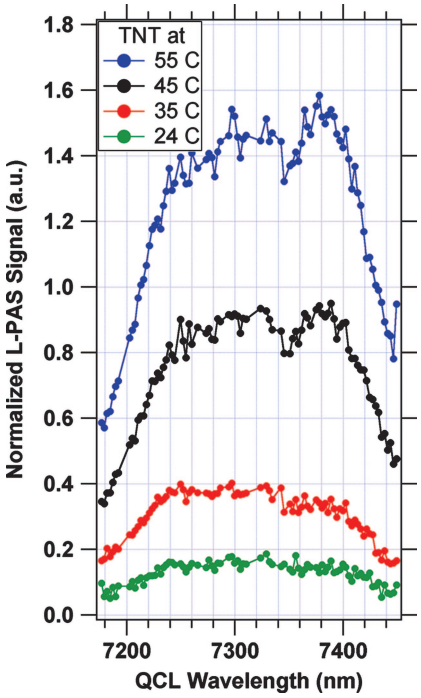

Fig. 5. Measured QCL-PAS absorption spectra of TNT at four different temperatures (see text for details).

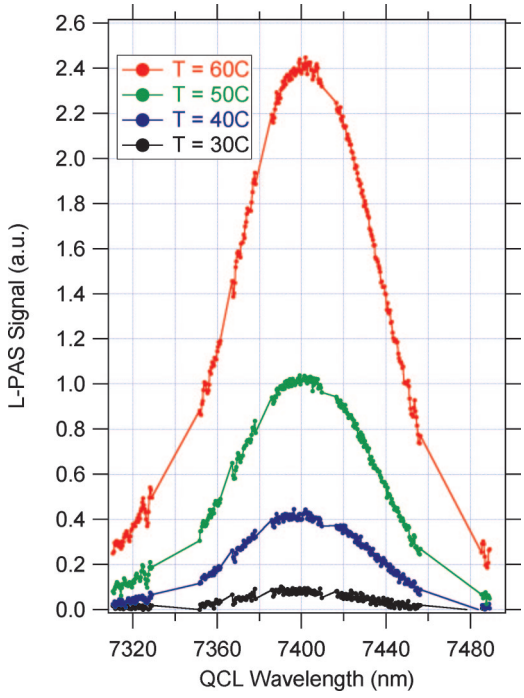

Fig. 6. QCL-PAS spectrum of purified TNT sample at three different temperatures using the smart grid tuning algorithm (see text).

acetylene. Fig. 4 shows the L-PAS peak as a function of acetylene concentration. From these data plotted in the top half of the figure, we estimate a 1σ detection capability of ≈2.5 ppb for acetylene.

Detection of TNT. For exploring detection of TNT, whose absorption spectrum (Fig. 1) shows a broad but strong absorption feature in the same wavelength region where PA detection data of acetylene are obtained in Fig. 3, we provided a continuous flow of CDA over a sample of TNT,[¶] and the emerging gas was continuously analyzed by our PA spectrometer. The temperature of the TNT sample could be controlled from RT to 60°C. The gas transport lines from the TNT sample chamber to the PA cell were maintained at 78°C and the PA cell was maintained at 60°C to prevent condensation of TNT vapors either in the transfer lines on in the PA cell. The upper temperature limit was set by the PA cell microphone, whose sensitivity begins to degrade significantly above 60°C but is not a limitation for future operation of the cell at higher temperatures using appropriate high-temperature microphones.

Fig. 5 shows an L-PAS spectrum obtained when the TNT sample was kept at 24°C, 35°C, 45°C, and 55°C, respectively. The PA spectrum qualitatively matches the shape of FTIR feature at 7,400 nm shown in Fig. 1. We comment on three specific aspects of the PA spectrum. The first is that a number of sharp absorption features arising from residual water vapor in the system (as verified by using water vapor absorption spectra obtained from HITRAN simulations) occur at certain wavelengths in the same region of wavelengths. These were avoided by using a "smart grid" of laser wavelengths that skips these specific wavelengths as the computer provides the tuning instructions to the EGC QCL.

The second is that the QCL-PAS spectrum is significantly broader than would be expected by looking at Fig. 1. In fact, the QCL-PAS spectrum consists of two distinct features, one centered at ≈7,380 nm that matches the expected absorption feature of TNT and the second centered at ≈7,300 nm that arises from the yet unknown impurity in the commercial-grade TNT. The unknown impurity was seen to be located on the surface of the TNT sample, and the 7,300-nm feature gradually disappeared as the TNT sample was kept at 100°C for 48 h while flushing the sample with CDA.

Fig. 6 shows the measured L-PAS spectrum of "purified" sample of TNT vapor in a background of room air with relative humidity of ≈40% at 25°C. The spectrum matches the expected position and width well. The spectra were taken by using 300 discreet wavelengths determined by the computer using the smart grid algorithm that skips the wavelengths corresponding to the known strong absorption features of water vapor. We conjecture that the disappearing peak at 7,300 nm could be used

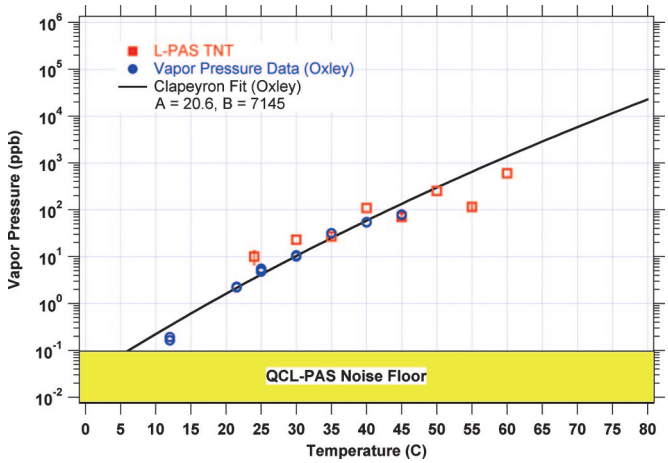

Fig. 7. Calculated vapor pressure of TNT (using Clapeyron fit) vs. temperature and the measured PA signal strength at various temperatures.

[¶]TNT samples (commercial grade) were obtained from Naval Air Warfare Center, Weapons Division (China Lake, CA). The pedigree of the samples is unknown.

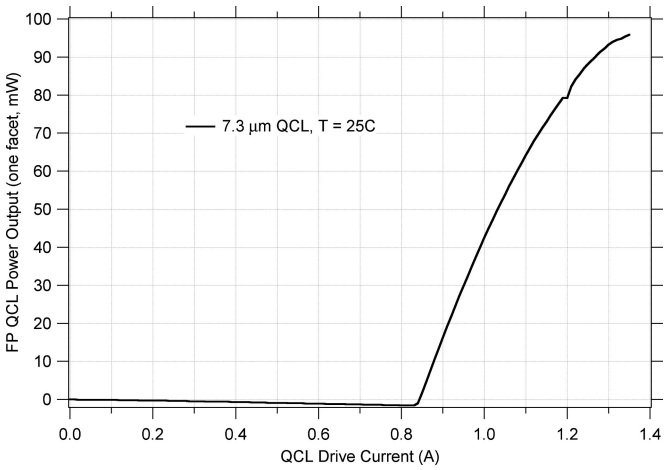

Fig. 8. Laser power vs. QCL drive current for the 7.3-μm gain chip operated in a Fabry–Perot geometry (the same chip used in the EGC geometry in these studies).

in the future to tag the origin and age of the TNT sample for forensic purposes. However, a confirmation of the conjecture will have to await getting samples of different age and origin from Naval Air Weapons Station China Lake (China Lake, CA). In either case, the shape and location information provides a powerful tool for QCL-PAS to uniquely identify TNT and minimize effects of interference.

The third aspect of the measured spectra (in Figs. 5 and 6) that deserves mention is that the signal feature in the ≈7,380 nm absorption region grows rapidly as the TNT temperature is increased from 24°C to 55°C as would be expected form the temperature dependence (ref. 8 and references therein) of the vapor pressure of TNT shown in Fig. 7. We have plotted the measured QCL-PAS data for TNT on the same plot, anchoring the 50°C QCL-PAS data on the vapor pressure vs. T plot. An acceptable correlation is seen between the vapor pressure data and the PA signal amplitude.

Sensitivity of TNT Detection. From the lowest temperature (24°C) at which the PA spectrum is shown, we can estimate the detection sensitivity from known vapor pressure data for TNT. The vapor pressure of TNT is seen to be (from Clapeyron fit curve) ≈3 ppb at 24°C (≈30 pg cm^{-3}). Comparing the L-PAS signal with the noise floor shown in Fig. 7, we estimate that we can detect TNT

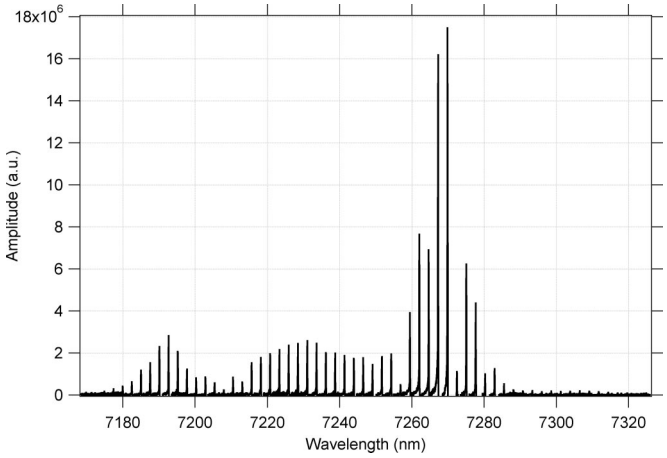

Fig. 9. FTIR analysis of the spectrum of the laser output (without the EGC geometry) with the drive current of 1.35 A.

at a level of 0.1 ppb (≈1.01 pg cm^{-3}) with a signal-to-noise ratio (S/N) of 1 (i.e., TNT at temperatures as low as 5°C). It should be noted, however, that the relationship of vapor pressure and temperature is dependent on the Clapeyron fit to the measured data.

Conclusions

The optical absorption shape information provided by QCL-PAS should permit easy discrimination between TNT and many interferents including nitroglycerine and other explosives as well as a host of commonly available fertilizers because the optical absorption reflects the chemical structure of the molecule rather than simple parameters such as overall mass or shape. QCL-PAS would provide high-sensitivity, low-false-positive detection of TNT desirable for many security-related applications. The compact size and relative simplicity of the operation of the QCL source should make QCL-PAS a preferred technique for looking for explosives in critical homeland security applications.

Materials and Methods

High-Power CW Operating RT QCLs. The 7.3-μm QCL epi material was grown using molecular-beam epitaxy by the Center for Quantum Devices (Northwestern University, Evanston, IL). After cleaving, the 3-mm-long, 10.6-μm-ridge-width chips were mounted epi-side down on AlN substrates by using Au–Sn eutectic solder (9). The chip carrier was maintained at 25°C by using a thermoelectric cooler (TEC). Heat was removed from the TEC by using a copper block maintained at 25°C. Operated in a Fabry–Perot geometry, the 7.3-μm QCLs (uncoated facets) generated multimode CW/RT power output of >80 mW (laser power vs. QCL drive current are shown in Fig. 8). The QCL power output was analyzed by using an FTIR spectrometer and is shown in Fig. 9. At the highest drive current, producing CW/RT power output of 80 mW, as expected we see a broad spectrum of power output when the QCL is operating in a Fabry–Perot geometry.

Continuous Tuning of EGC QCLs. To produce a single frequency laser output that is conveniently tunable over the broad spectral region represented by the gain features of the QCL chip (and as seen in Fig. 9), the QCL gain chips, with uncoated facets, were incorporated into an EGC setup with the total length of the external cavity of 4 cm with appropriate beam expanding and collimating 4-mm-diameter f/0.7 aspheric antireflection coated ZnSe collimating lenses. The grating incidence angle could be precisely and reproducibly adjusted by using a computer-controlled linear actuator with an integrated encoder. The grating position and therefore the length of the EGC were accurately controlled by using another linear piezoelectric linear actuator.

The principal differences between the QCL wavelength tuning scheme described earlier (10) and the present work arise from the much shorter external cavity length (25 vs. 100 cm) and the center frequency of the gain curve of the QCL gain chip (7.3 vs. 6.3 μm). The shorter external cavity length and the different refractive index of the gain chip compared with that used in ref. 10 require different numerical values of tuning constants that were obtained through characterizing the output of the EGC-QCL with a high-resolution FTIR spectrometer. Continuous, mode hop free, real-time tuning was accomplished by a computer-controlled algorithm that simultaneously adjusted the grating angle, the external cavity length, and the QCL drive current.

We obtained an overall tuning range of ≈350 nm centered around 7,350 nm (Fig. 2), with highest single frequency optical power of nearly 200 mW. (Note that the CW/RT EGC QCL power output is nearly twice the CW/RT Fabry–Perot QCL power output shown in Fig. 8 because the Fabry–Perot output shows the output

per each facet. The external grating reflection feedback to one facet of the QCL in the external grating geometry improves the operating characteristics of the QCL by reducing the total optical loss inside the laser cavity and provides all of the QCL output from one facet.) Continuous tuning was demonstrated by recording output spectra over the entire spectral tuning range by using a high-resolution FTIR. The FTIR spectra, in their highest resolution mode, provided information about the linewidth of the EGC QCL, which was <600 MHz limited by the FTIR resolution. A convincing proof of continuous tuning over a significant range of the tuning range and maintenance of the very narrow output linewidth while tuning was obtained by measuring a QCL-PAS spectrum of 10 ppm acetylene in 300 torr of CDA as described earlier and shown in Fig. 3. The near perfect match between the measured line positions and the linewidths with those obtained from a HITRAN simulation provides convincing proof that the computer-based algorithm produces a mode hop free tuning even with uncoated facet QCL chip. High-quality antireflection coating (11) on the external grating side of the chip would essentially eliminate many of the complexities of the computer-based tuning algorithm and increase the tuning range of this QCL gain chip.

We thank the Naval Air Warfare Center, Weapons Division (China Lake, CA) for providing the TNT samples used in these studies. This work was supported in part through Defense Advanced Research Projects Agency Contract HR0011-04-C-0102 (Approved for Public Release, Distribution Unlimited).

1. Webber ME, Pushkarsky MB, Patel CKN (2005) *J Appl Phys* 97:113101.
2. Pushkarsky MB, Webber ME, Macdonald T, Patel CKN (2006) *Appl Phys Lett* 88:044103.
3. Claspy PC, Pao Y-H, Kwong S, Nodov E (1976) *App Opt* 15:1506–1509.
4. Pushkarsky MB, Webber ME, Patel CKN (2003) *Appl Phys B* 77:381–385.
5. Crane RA (1978) *Appl Opt* 17:2097–2102.
6. Todd MW, Provencal RA, Owano TG, Paldus BA, Kachanov A, Vodopyanov KL, Hunter M, Coy SL, Steinfeld JI, Arnold JT (2002) *Appl Phys B* 75:367–376.
7. Rothman LS, Barbe A, Benner DC, Brown LR, Camy-Peyret C, Carleer MR, Chance K, Clerbaux C, Dana V, Devi VM, et al. (2003) *J Quant Spectrosc Radiat Transfer* 82:5–44.
8. Oxley JC, Smith JL, Shinde K, Moran J (2005) *Propellants Explosives Pyrotechnics* 30:127–130.
9. Tsekoun A, Go R, Pushkarsky MB, Razeghi M, Patel CKN (2006) *Proc Natl Acad Sci USA* 103:4831–4835.
10. Pushkarsky MB, Tsekoun A, Dunayevskiy IG, Go R, Patel CKN (2006) *Proc Natl Acad Sci USA* 103:10846–10849.
11. Maulini R, Mohan A, Giovannini M, Faist J, Gini E (2006) *Appl Phys Lett* 88:201113-1–201113-3.